Minority Carrier Injection in High-Barrier Si-Schottky Diodes

Gaurav Gupta, Satadal Dutta, *Student Member, IEEE*, Sourish Banerjee, and Raymond J. E. Hueting, *Senior Member, IEEE*

***Abstract*—In this paper, we investigate the presence of minority carriers and their role in charge carrier transport in silicon (Si) Schottky diodes with a high potential barrier. Using TCAD simulations along with an analytical model, we show that an inversion charge is induced at the metal–semiconductor (MS) interface in a high-barrier Schottky diode which imparts bipolar-type current characteristics to otherwise a unipolar Schottky diode, even at low-injection operation. In such a high-barrier diode, minority diffusion also becomes important along with the majority carrier thermionic emission and therefore cannot be neglected, unlike in a conventional Schottky diode. The presence of minority carriers at low injection in a high-barrier Si Schottky diode has been experimentally verified via a prior-reported two-diode electrical test method, reverse recovery measurements, and by measuring infrared electroluminescence. It is also shown, via TCAD simulations, that the diffusion component becomes more pronounced in case of a reduced Gummel number and at elevated temperatures.**

***Index Terms*—Diffusion, electrostatic doping, metal work function, minority carriers, p-n junctions, Schottky barrier (SB), shallow junctions, silicon, thermionic emission (TE).**

I. Introduction

CONVENTIONAL impurity doping of semiconductor devices has become more challenging for nanometer-scale devices with an extremely high doping gradient [1], [2]. Moreover, impurity doping is also not yet technologically matured for emerging material systems other than silicon (Si) such as wide bandgap semiconductors (e.g., GaN, SiC, and ZnO), carbon nanotubes [3]–[6], and emerging 2-D materials (graphene, phosphorene, silicone, and transition metal dichalcogenides) [7], [8], which are increasingly relevant for future electronic as well as optoelectronic devices. From this viewpoint, electrostatic doping ([9] and references therein) is being extensively investigated to overcome the challenges of conventional doping approaches in dimensionally scaled devices.

In this direction, the case of a shallow p-n junction induced by a metal with a suitable work function in a 1-D Schottky diode was previously discussed [9]–[11]. In conventional Schottky barrier (SB)-based devices, the current is governed by one or more Schottky contacts. The physics of an SB formed at the metal–semiconductor (MS) interface has been well described earlier [12]. There is a prevalent perception that at low injection, the SB diode is a majority carrier unipolar device in which the current is solely governed by thermionic emission (TE) (see [13]). However, this is not necessarily valid in case of a high-barrier ($q\phi_b > 0.5E_g$) Schottky diode, where ϕ_b is the SB height, E_g is the bandgap, and q is the elementary charge. For this case, excessive band bending near the MS interface will result in charge carrier inversion and consequently a more efficient emitter. This will transform an otherwise unipolar Schottky device into a (bipolar) p-n junction type device. An analytical model and the limiting conditions for strong inversion (thus bipolar behavior) at a 1-D Schottky electrode were derived before [9]. The model indicates that for a suitable metal work function (ϕ_m) that governs ϕ_b, the charge carriers of the opposite polarity to that of the substrate doping are induced near the MS interface. Such approach of electrostatically realizing shallow p-n-type junctions could be relevant for future CMOS ultrathin body (UTB) devices where conventional impurity doping is a challenge. Recently, TCAD simulation studies on such 1-D Schottky junctions have been reported for a bipolar transistor [10] and a tunnel diode [9]. Such junctions can also be used for realizing light-emitting devices without the need for chemically doped p-n junctions.

Metal-induced inversion charge using a Schottky electrode was first speculated by Brattain and Bardeen [14] in their point-contact Ge rectifier from their observed bipolar-like amplification. Thereafter, there have been no reports on experimental investigation of this concept. In the past, Wittmer [15], [16] reported high-SB diodes using silicided contacts on bulk Si and analyzed the conduction mechanisms of such diodes. Such high ϕ_b (reported 0.982 V for IrSi/Si) would result in inversion charge, and therefore, it is anticipated that some deviation from the TE model should have been observed. However, the author concluded that the measured current fully obeyed a single-carrier TE theory in the range 200–300 K

Manuscript received November 23, 2017; revised January 24, 2018; accepted February 15, 2018. Date of publication March 2, 2018; date of current version March 22, 2018. This work was supported by the NWO Domain Applied and Engineering Sciences (TTW), The Netherlands (OTP 2014), under Project 13145. The review of this paper was arranged by Editor K. Kalna. *(Corresponding author: Gaurav Gupta.)*

The authors are with the MESA+ Institute for Nanotechnology, University of Twente, 7500AE Enschede, The Netherlands (e-mail: g.gupta@utwente.nl).

Color versions of one or more of the figures in this paper are available online at http://ieeexplore.ieee.org.

Digital Object Identifier 10.1109/TED.2018.2807926

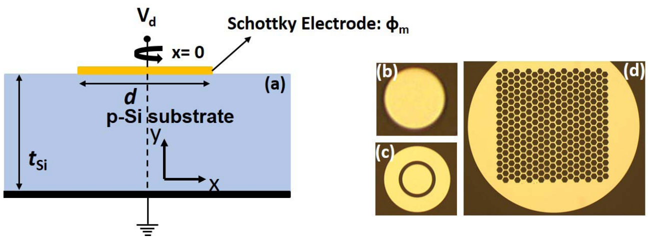

Fig. 1. (a) Schematic cross section of the experimental and TCAD simulated device. Optical micrographs (not to the same scale) of fabricated devices: (b) Circular electrode with diameter $d = 100$ μm, (c) Ring geometry as used for the two-diode test method, (d) Hexagonal openings (side $a = 10$ μm) in the circular electrode ($d = 550$ μm) used for IR light emission measurements.

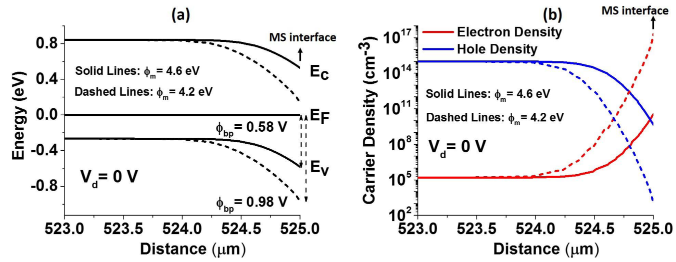

Fig. 2. (a) Simulated band-diagrams and (b) charge carrier profiles for a Schottky diode with a metal work function $\phi_m = 4.6$ eV and $\phi_m = 4.2$ eV. The origin of the x-axis (distance) is located at the bottom of the substrate.

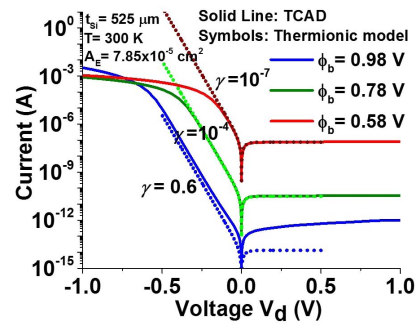

Fig. 3. Simulated I–V characteristics of Schottky diodes for different values of ϕ_b (ϕ_m). γ is calculated at -0.2 V (forward bias).

and did not consider the possibility of (minority) diffusion. A possible reason for this could have been the use of a bulk Si substrate which actually diminishes the contribution of the diffusion component as we discuss further in this paper. Also, measurements beyond 300 K were not reported where diffusion would have become relatively more noticeable.

In this paper, we perform extensive TCAD simulations and experimental investigations on the presence of minority carriers and their role in the conduction in a high-ϕ_b Schottky diode. This paper is organized as follows. In Section II, we first investigate the conduction mechanism of p-Si Schottky diodes with different ϕ_m electrodes using TCAD simulations. In Section III, we present experimental results of high-ϕ_b Al/p-Si Schottky diodes and compare them with TCAD simulations. In Section IV, we discuss the technological applications of such Schottky-based junctions along with some practical considerations. Finally, the conclusions are drawn in Section V.

II. TCAD Simulation

Fig. 1(a) shows the test structure that has been investigated via TCAD simulations in Sentaurus Device [17]. We have used a p-type Si-substrate with thickness t_{Si} of 525 μm and a doping level N_a of 10^{15} cm^{-3}. For such doping, a $\phi_m < 4.34$ eV will result in surface inversion as derived in [9] and possibly a p-n-type operation, while $\phi_m \geq 4.6$ eV will result in a typical Schottky-type operation (i.e., unipolar majority carrier transport). Therefore, we adopt Schottky metal work functions between 4.2 (p-n-type operation) and 4.6 eV (Schottky) for our simulation study. For computation efficiency, a 2-D Delaunay mesh with triangular elements was used. The minimum mesh spacing near the MS interface in the center of the device was $\sim$7 μm in the x-direction and $\sim$7 nm in the y-direction. Also, for comparing with experiments, a cylindrical symmetry was incorporated around the y-axis to solve the Poisson and continuity equations. Fermi–Dirac statistics along with the Philips unified mobility model [18] were used. For recombination, doping and temperature-dependent Shockley–Read–Hall and Auger models [17] were included. Initially, ideal interfaces are assumed for the conceptual understanding of the device operation. Then, the effect of interface traps is discussed.

Fig. 2 shows the simulated band diagram and charge carrier profile, both in equilibrium condition, for two different ϕ_m. The use of $\phi_m = 4.6$ eV results in a typical Schottky condition with a depletion region at the interface and ϕ_b of 0.58 V. However, $\phi_m = 4.2$ eV results in aggressive band bending at the interface with ϕ_b of 0.98 V. In this case, the Fermi level at the interface is close to the conduction band, implying surface inversion with a peak-induced electron concentration of $\sim 10^{17}$ cm^{-3}.

Fig. 3 shows the simulated I–V characteristics of such Si p-type Schottky diodes for three different ϕ_b (ϕ_m). The conduction for the low $\phi_b = 0.58$ V ($\phi_m = 4.6$ eV) is solely governed by TE of majority carriers as evident from the excellent agreement of TCAD (both forward and reverse currents), with an analytical TE I–V model [19]. For moderate $\phi_b = 0.78$ V ($\phi_m = 4.4$ eV), the majority hole current via TE is still dominant. However, a clear deviation from the TE theory is observed for the high $\phi_b = 0.98$ V ($\phi_m = 4.2$ eV). The TE theory only accounts for the hole current component. The extra current component is attributed to the presence of electron (minority carrier) diffusion. In this case, the electron diffusion current (I_e) is comparable to the TE hole current (I_h) and contributes significantly to the total current ($I = I_e + I_h$) as indicated by a high minority carrier injection ratio γ (I_e/I) [19] in Fig. 3. The significantly higher reverse leakage current than predicted by the TE model in the case of the high-ϕ_b diode is also attributed to diffusion [Fig. 4(a)]. This bipolar conduction is in contrast to the prevalent perception where SB diodes are considered to be majority carrier unipolar devices at low injection [19], [20].

Fig. 4(a) shows the electron current (I_e) components of the simulated I–V curves (Fig. 3) for varying ϕ_b. The diffusion

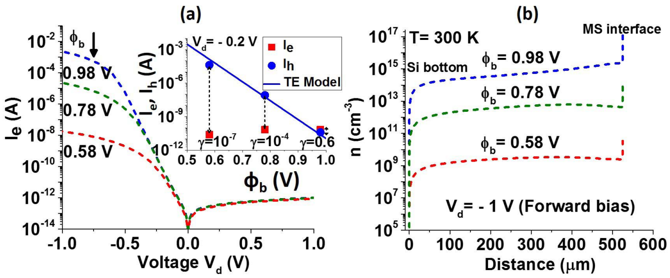

Fig. 4. (a) Electron current components (I_e) of the simulated I–V characteristics of Fig. 3 at different values of ϕ_b (inset: I_e and I_h for varying ϕ_b at a fixed forward bias $V_d = -0.2$ V). (b) Simulated electron (minority carrier) profile across the device at $V_d = -1$ V forward bias for different values of ϕ_b.

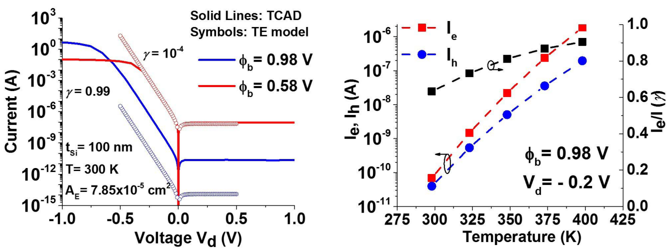

(a) (b)

Fig. 5. (a) Simulated I–V characteristics of a Schottky diode with $t_{\mathrm{Si}} =$ 100 nm for both high-ϕ_b and low-ϕ_b diodes and (b) I_e and I_h against the temperature for the high-ϕ_b diode ($V_d = -0.2$ V, t_{Si} = 525 μm).

component I_e, being governed by the Gummel number of the substrate ($G_b = \int_0^{t_{\mathrm{Si}}} N_a(x)dx$) [21], remains unchanged with varying ϕ_b in the exponential region of the I–V curves. However, γ [see inset in Fig. 4(a)] varies with ϕ_b because the latter affects I_h. Therefore, I_e can be neglected for a low-ϕ_b (low γ) diode but cannot be ignored for a high-ϕ_b (high γ). It is also known that the series resistance of a Schottky diode is higher than that of a p-n junction diode [20] because of the poor supply of minority carriers [see Fig. 4(b)]. For $\phi_b = 0.58$ and 0.78 V, the minority carrier concentration is still below N_a and, therefore, does not affect the overall series resistance much. However, in the case of an extreme $\phi_b = 0.98$ V, the minority carrier concentration is comparable to N_a that lowers the series resistance. The effect of ϕ_b on the series resistance can be observed from the I–V plots in Figs. 3 and 4(a) at higher biases ($V_d = -1$ V, forward) where the current increases with ϕ_b.

The diffusion current can be further tuned by changing the Gummel number of the substrate. By reducing t_{Si} from 525 μm to 100 nm, γ increases from 0.6 to 0.99 for $\phi_b =$ 0.98 V as shown in Fig. 5(a). Here, a larger deviation from the TE model is observed implying that the current is largely diffusion dominated. However, varying t_{Si} does not affect the TE majority current, and therefore, the current for a device with $\phi_b = 0.58$ V is still following the TE model. The pronounced effect of the diffusion current in high-ϕ_b diodes could be relevant for advanced UTB devices while it may be unnoticeable for bulk devices [15], [16].

Also the temperature dependence of diffusion is higher than that of TE because of the relatively high potential barrier in

TABLE I
SUMMARY OF TCAD SIMULATION RESULTS FOR VARIOUS ϕ_b, SUBSTRATE THICKNESSES, AND TEMPERATURES ($V_d = -0.2$ V)

ϕ_b(V)	T(K)	t_{Si}(μm)	γ	Conduction mechanism
0.58	298	525	10^{-7}	TE
0.58	298	0.1	10^{-4}	TE
0.78	298	525	10^{-4}	TE
0.98	298	525	0.6	Minority Diffusion, TE
0.98	298	0.1	0.99	Minority Diffusion
0.98	398	525	0.9	Minority Diffusion

the case of the former [19]. Therefore, for the high-ϕ_b diode, γ increases with the temperature as shown in Fig. 5(b). Such a rise in the diffusion current at higher temperatures was also observed experimentally in our Schottky diodes as we discuss in Section III. Table I summarizes the results for various ϕ_b.

III. EXPERIMENTAL RESULTS

p-Si Schottky diodes were fabricated using Al as a top electrode (Fig. 1). The choice of Al is based on its reported low vacuum work function ϕ_m of 4.28 eV which ideally will result in ϕ_b of 0.89 V ($q\phi_b = E_g - \phi_m + \chi_s$), where E_g is the Si bandgap (1.12 eV) and χ_s is the Si electron affinity (4.05 eV). The substrate was utilized as the bottom electrode. A (111) p-type Si substrate with N_a of 10^{15} cm^{-3} and with a native oxide was used. A 200-nm Al was sputtered on the polished surface. The electrodes were then patterned using a standard photolithography process using a positive photoresist. The presence of the thin native oxide between Al and Si surface avoids chemical interdiffusion and also decouples the electron states in the Si from the metal [12], [22], which might lower the effective ϕ_b. We also avoided annealing the wafer to prevent alloy formation and to keep the as-deposited metallurgical nature of the junction intact. As a reference, to obtain a low-ϕ_b diode, an n-Si/Al wafer was also fabricated following a similar process.

Temperature-dependent I–V measurements of the fabricated Al/p-Si Schottky diodes were done using a Keithley 4200 Semiconductor Characterization System with a preamplifier enabling DC measurements with a combined noise level of ~10 fA for an integration time of 100 ms. The measurements were performed under dark conditions and on a temperature controlled chuck. A moderately high ϕ_b of 0.77 V with an ideality factor n of 1.09 was extracted from the Richardson plot [see Fig. 6(a)] in the exponential region ($V_d = -0.2$ V) of the I–V curves. The extracted ϕ_b from I–$V(T)$ measurements is also in agreement with that obtained from C–V measurements as shown in Fig. 6(c). The relatively low value of the extracted A^* (4.06 Acm^{-2}K^{-2}) compared to the reported value of 32 ±2 Acm$^{-2}K^{-2}$ [19], [23] for a p-Si substrate can be partly due to the inhomogeneity at the interface [24] as a result of the unannealed electrical contacts. Further, the nonideality of n ~1.09 could be attributed to the presence of the interfacial layer (native oxide) and image force effect [19]. However, since the effective $\phi_b > 0.5E_g/q$, some level of surface inversion is expected in this diode.

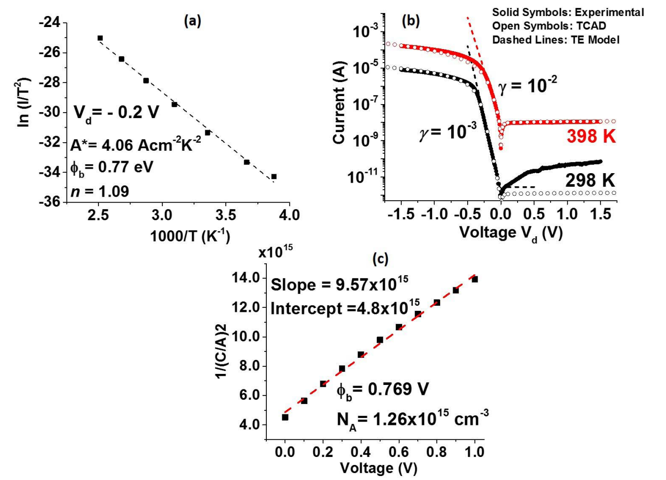

Fig. 6. (a) Richardson plot of the fabricated Al/p-Si diode ($A_e = 7.85 \times 10^{-5}$ cm^2) at $V_d = -0.2$ V forward bias. ϕ_b of 0.77 V was extracted using this measurement. (b) Measured *I*–*V* at $T = 298$ K and $T = 398$ K and their fitting using TCAD simulation and analytical TE model with experimentally extracted values of ϕ_b, Richardson's constant A^*, and ideality factor *n*. (c) ϕ_b extraction from *C*–*V* analysis in reverse bias.

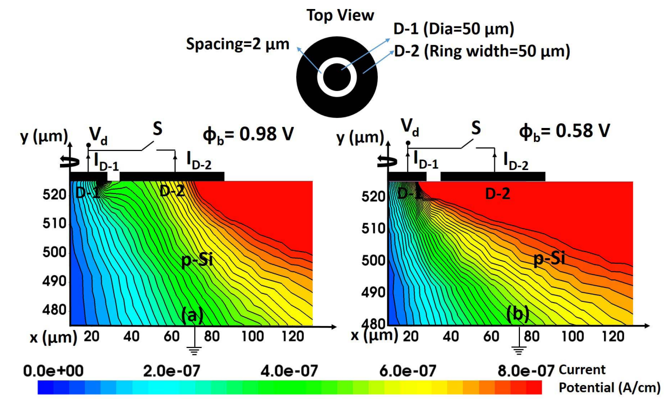

Fig. 7. Schematic of the two-diode test method and measurement configuration with TCAD simulated current flow lines. The flow lines indicate the current spreading in the device when only $D-1$ is biased (forward current bias = 1 μA) for case (a) $\phi_b = 0.98$ V and (b) $\phi_b = 0.58$ V. The current spreading due to minority carrier injection is observed near the contact for the high-ϕ_b diode, while less current spreading was observed for the low-ϕ_b diode. The switch *S* is in closed position when both $D-1$ and $D-2$ are biased.

Similar measurements on the n-Si/Al diode results in a low ϕ_b of 0.53 V as desired for the comparison.

The extracted ϕ_b of 0.77 V was used as an input for the TCAD simulation where excellent agreement with the experimental data was obtained in forward bias, as shown in Fig. 6(b). ϕ_b of 0.77 V results in a downward band bending near the MS interface with a peak-induced electron concentration of 3×10^{13} cm^{-3}. Note that this induced electron concentration for the moderately high experimental ϕ_b of 0.77 V is much lower than that for the extremely high ϕ_b of 0.98 V ($\phi_m = 4.2$ eV) adapted for simulations in Section II. Therefore, less pronounced effects on the conduction are expected. Consequently, in our experimental devices, the current is largely dominated by TE majority carriers, i.e., holes, with $\gamma = 10^{-3}$. This is further evident as experimental and TCAD *I*–*V* characteristics are in agreement with the TE analytical model. We also considered the possibility of majority carrier diffusion along with TE as described by the thermionic-emission-diffusion theory [19], [25]. At *T*=298 K, we estimated that the effective thermionic recombination velocity ($v_{\rm R}$) $\ll$ effective diffusion velocity (v_d). This implies that the majority carrier current can essentially be described by the TE theory only. Furthermore, as checked in TCAD, the hole quasi-Fermi level $E_{\rm Fp}$ was essentially flat throughout the depletion region which also suggests that the TE model for majority carriers is applicable. The relative contribution of the electron diffusion though increases at higher temperatures to $\gamma = 10^{-2}$. However, *J* is still governed by TE. Therefore, in this case, it is not straightforward to establish the presence of minority carriers experimentally.

To study the influence of minority carrier injection in a high-ϕ_b diode, a prior reported two-diode method [26], [27] was adopted. With this technique, it is possible to distinguish the operation of a (Schottky-based) shallow p-n junction diode from that of a conventional Schottky diode at low injection.

The schematic of the two-diode test method is illustrated in Fig. 7 where two similar diodes, $D-1$ and $D-2$, are closely spaced (~ 2 μm). Here, the current of $D-1$ is measured when it is operated in single mode and in parallel mode along with $D-2$. In the case of a p-n-type diode, there will be a significant contribution of minority carrier injection from the contacts (high γ), and as a result, the current will spread outward from the contacts. When $D-1$ is operated in parallel with $D-2$, then in the case of p-n-type diodes, the current of each diode will be less compared to that in single-mode operation due to influence of current spreading from the neighboring diode. This influence can be measured from the differential current level in the exponential part of the *I*–*V* curve. While in the case of a conventional Schottky diode, the minority carrier injection will be insignificant, and therefore, there will be hardly any current spreading near the contacts. Hence, in the case of conventional Schottky diodes, the current for both modes (i.e., single-mode and parallel-mode operations) will be the same, as it is governed by majority carrier injection from the substrate and depends only on the area of the diode. Therefore, then hardly any influence of the neighboring diode will be noticeable in the exponential part of the *I*–*V* curve.

Fig. 8 shows the TCAD simulated electron (I_e) and hole (I_h) currents in the case of high-ϕ_b Schottky diodes when diode $D-1$ is operated in single mode ($I_{\rm D-1}$) and in parallel mode ($I_{\rm D-1'}$) with diode $D-2$. Only the minority (electron) current is affected in parallel-mode operation, while the majority current remains unaffected. Since in the case of a high-ϕ_b diode, γ is high, this influence can be measured in the two-diode test configuration.

Fig. 9(a) and (b) shows the experimental two-diode characteristics for two different ϕ_b diodes. For the p-Si/Al diode with $\phi_b = 0.77$ V, a slight decrease in the diode $D-1$ current ($\Delta I = I_{D-1} - I_{\rm D-1'}$) in the exponential part of the plot when operated in parallel with diode $D-2$ was observed as shown in Fig. 9(a). Here, a current discrepancy ($\Delta I/I$)

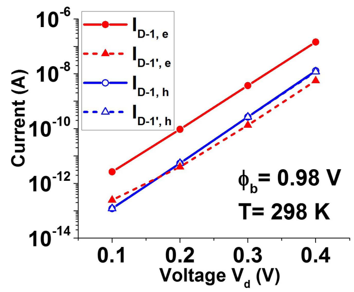

Fig. 8. Simulated electron (I_e) and hole (I_h) currents of diode $D-1$ when operated in single mode (I_{D-1}) and in parallel mode ($I_{D-1'}$) in case of high ϕ_b (= 0.98 V) Schottky diodes. t_{Si} = 525 μm and $N_a = 10^{15}$ cm^{-3}.

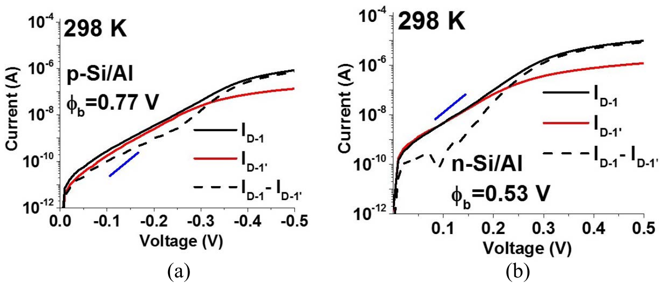

Fig. 9. I–V curves showing the measured $D-1$ current when operated in single mode and parallel mode at 298 K for (a) ϕ_b = 0.77 V and (b) ϕ_b = 0.53 V. Blue solid line: ideality factor $n = 1$ for reference.

of 37 % was observed in the forward bias exponential region at $V_d = -0.1$ V. This indicates the influence of minority carrier (electron) injection in the p-type Schottky diode. However, in the case of the n-Si/Al diode with a near midgap ϕ_b = 0.53 V, the influence of the minority carrier injection from the metal side into the semiconductor is negligible, and therefore, the $D-1$ current remains unaffected as shown in Fig. 9(b). Here, a current discrepancy ($\Delta I/I$) of less than 7% was observed at V_d = 0.1 V. Further, the influence of current spreading increases at higher temperatures where a higher $\Delta I/I$ = 51 % was noted at 398 K in the case of diodes with ϕ_b = 0.77 V. This is expected as an increase in temperature increases the diffusion component more than the TE current, and therefore, will raise γ, in this case, by one order of magnitude, as observed in our TCAD simulations [Fig. 5(b)]. The observed lower $I_{D-1'}$ in the series resistance regime for both diodes in Fig. 9(a) and (b) is due to the high resistance encountered during parallel-mode operation [26], [27].

The presence of minority charge carriers in high- ϕ_b diodes was also observed via reverse recovery measurements [28] as shown in Fig. 10(a) for both ϕ_b diodes. We measured a 42% higher stored charge ($Q_s = 4.54 \times 10^{-8}$ C/cm^2) in our p-Si/Al diode with a ϕ_b = 0.77 V compared to our n-Si/Al diode with a ϕ_b = 0.53 V. Interestingly, the presence of a lower Q_s and consequently higher resistivity for Si Schottky diodes with ϕ_b < 0.8 V has been highlighted before in [29]. Q_s is much higher in the case of an extreme ϕ_b as shown with TCAD simulations in Fig. 10(b).

Further, the presence of a minority carrier component, although relatively small, should also result in electroluminescence (EL) in Si via band-to-band recombination in high- ϕ_b Schottky diodes, which otherwise is unexpected at low injection from a conventional (unipolar) Schottky diode. Therefore, we also performed EL measurements in our diodes. A cooled InGaAs detector-based camera (XEVA-320 from Xenics) with a spectral detection range of 950–1700 nm was used for capturing the EL micrograph using an integration time of 30 s. Low-intensity light emission in the infrared (IR) range was observed from our p-Si/Al diodes (ϕ_b = 0.77 V) at a constant current drive of 20 mA (J ~25 A/cm^2) at room temperature, as shown in Fig. 11(a).

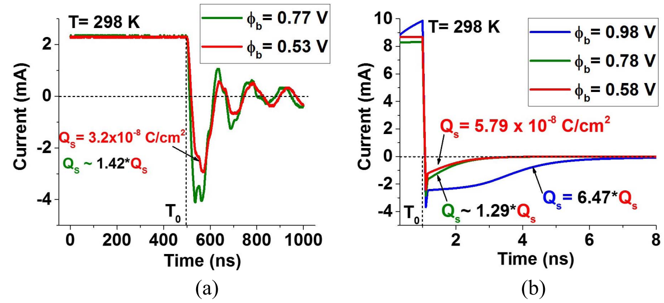

Fig. 10. (a) Reverse recovery measurements of the diodes ($A_e = 5.96 \times 10^{-3}$ cm^2) with different values of ϕ_b showing current versus time plot when diode is suddenly switched from a forward-bias state to a reverse-bias state at time T_0 by applying a voltage pulse. (b) Simulated reverse recovery characteristics for the similar devices ($A_e = 7.85 \times 10^{-5}$ cm^2) with different values of ϕ_b.

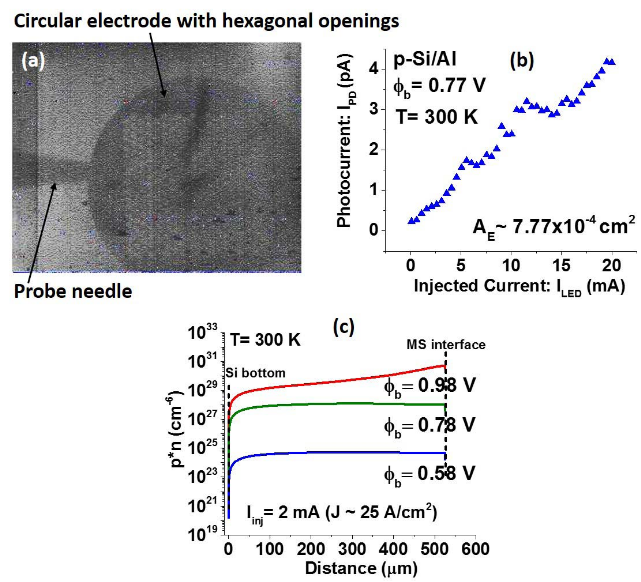

Fig. 11. (a) EL IR micrograph (in grayscale) of our fabricated p-Si/Al circular diode (ϕ_b=0.77 V) with hexagonal openings [see Fig. 1(d)]. A faint glow (white regions) was observed using IR camera from the hexagonal openings and from the periphery of the circular electrode. (b) Measured short-circuit current (I_{PD}) in the external PD versus injected forward current (I_{LED}) for the same p-Si/Al diode. (c) Simulated p-n product at injected current density $J \sim$ 25 A/cm^2 for different values of ϕ_b. The p-n product increases with ϕ_b as expected.

In addition, we also measured the emitted light via the short-circuit current (I_{PD}) of an off-chip Si-photodiode (PD) [30] as shown in Fig. 11(b). The I_{PD} is proportional to the emission intensity that rises steadily with injected current I_{LED} of the high-ϕ_b Schottky diode. However, no measurable light

TABLE II
SUMMARY OF EXPERIMENTAL RESULTS

Diode	ϕ_b(V)	2-diode test	Reverse Recovery	EL
p-Si/Al	0.77	$\Delta I/I$=37 %	Q_s=4.54x10^{-8} C/cm^2	Yes
n-Si/Al	0.53	$\Delta I/I$=7 %	Q_s=3.2x10^{-8} C/cm^2	No

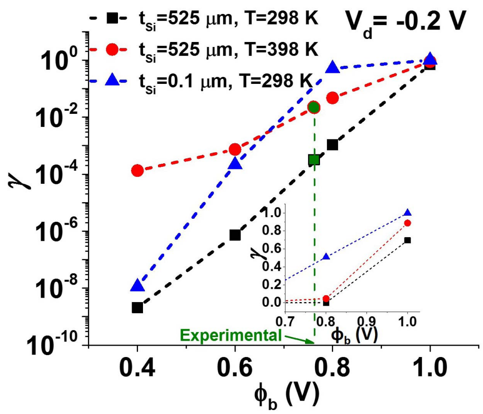

Fig. 12. Simulated minority carrier injection ratio γ as a function of the barrier height (ϕ_b) of the p-Si Schottky diode for different substrate thicknesses and temperatures. Inset: same plot in linear scale at higher ϕ_b. γ is calculated at $V_d = -0.2$ V forward bias. Green dashed line: our experimentally measured ϕ_b for a 525-μm-thick substrate.

emission (I_{PD}) was observed from the lower ϕ_b (0.53 V) n-Si/Al diode due to the relatively low minority carrier injection. The maximum injected current density of $J \sim 25$ A/cm^2 is at low injection ($J \ll qNv_{sat} = 1.6 \times 10^3$ A/cm^2, where N is the active doping concentration and v_{sat} is the saturation velocity). It is commonly known that at high-injection minority carriers do play a role even in a conventional Schottky diode [19], [31], [32]. However, the observation of light emission from the Schottky diode at low injection indicates the presence of minority carriers which is also in agreement with our simulations. The emitted light intensity that is proportional to the *p-n* product [33], [34] increases for a higher ϕ_b as shown in Fig. 11(c). The *p-n* product hence the recombination rate is highest near the MS interface. Unfortunately, in our experiment, the moderately high ϕ_b and the indirect Si bandgap make EL from this diode too weak to be detected by our spectrometer. Also, because of the unannealed contacts for the reason discussed earlier, we suspect that the ϕ_b is susceptible to change with the injected current due to local heating. This also makes the detection of a very low-intensity emission difficult in our devices. For a stronger emission, an extreme ϕ_m that can result in a very high ϕ_b ($q\phi_b > 0.5E_g$) should be employed. The results of our experimental investigations are summarized in Table II, all indicating the presence of minority carriers in the high-ϕ_b diode.

IV. DISCUSSION

Fig. 12 summarizes the ϕ_b dependence of the relative contribution of the diffusion component. As discussed earlier, for a high-ϕ_b Schottky diode, minority carrier diffusion is important and, therefore, cannot be neglected particularly for reduced substrate thicknesses or a reduced Gummel number in general, and higher temperatures.

The pronounced effect of the minority carrier transport in high-ϕ_b Schottky diodes at reduced substrate thicknesses could be attractive for next generation dimensionally scaled CMOS devices where conventional doping is a challenge. There such Schottky-based junctions can be used to realize, for instance, tunnel devices [11] or even low-intensity light emitters for applications such as on-chip communication [35]. In addition, a Schottky-based p-n-type junction could be relevant for optoelectronic applications (for example, Schottky-based UV LEDs [36]) in direct bandgap materials such as GaN, where conventional doping is also not well matured.

From a technological viewpoint, the effect of interface traps cannot be ignored for realizing a high-ϕ_b Schottky diode. Interface traps influence ϕ_b [12], [19] and particularly in covalent semiconductors, it is only weakly dependent on ϕ_m as the Fermi level is pinned at the interface by a large density of surface states. The effective ϕ_b would reduce from its ideal value in presence of interface traps, which in turn would decrease the induced inversion charge concentration near the MS interface [9]. Consequently, minority carrier transport would become less important. Interestingly, for ionic semiconductors such as GaN, CdS, and ZnS, the Fermi-level pinning effect is less pronounced and ϕ_b should strongly depend on ϕ_m [19].

The use of a thin interfacial tunneling layer has also been proposed earlier to gain better control over a resultant ϕ_b and thus induced inversion charge [9], [22], [37]–[39]. Interestingly, interfacial layers can further be utilized to tune the diffusion current in a high-ϕ_b diode [19].

V. CONCLUSION

We have discussed the presence of the otherwise negligible minority carrier diffusion in high-barrier ($q\phi_b > 0.5E_g$) Schottky diodes at low injection using TCAD simulations and experiments. TCAD simulations indicate that in a high-barrier Schottky diode, the presence of the induced inversion charge carriers near the MS interface imparts p-n junction-type bipolar current characteristics to otherwise a unipolar Schottky diode. In the case of a high-barrier diode, minority carrier diffusion is important and therefore cannot be neglected. The contribution of diffusion in such a diode can further be increased by reducing the substrate thickness (Gummel number in general) and increasing temperature. The observed IR emission in low-injection condition, higher stored charge during reverse recovery, and current spreading near the Schottky contact using the two-diode test methodology indicate the influence of minority carrier diffusion in such high-barrier Schottky diode, which otherwise is negligible in a conventional Schottky diode.

ACKNOWLEDGMENT

The authors would like to thank Prof. L. K. Nanver and Prof. J. Schmitz for critically reading this paper and fruitful discussions on the subject.

References

[1] E. C. Jones and E. Ishida, "Shallow junction doping technologies for ULSI," *Mater. Sci. Eng. R, Rep.*, vol. 24, no. 1, pp. 1–80, 1998.

[2] P. S. Peercy, "The drive to miniaturization," *Nature*, vol. 406, no. 6799, pp. 1023–1026, 2000.

[3] W. Walukiewicz, "Intrinsic limitations to the doping of wide-gap semiconductors," *Phys. B, Condens. Matter*, vols. 302–303, pp. 123–134, Jan. 2001.

[4] P. Kozodoy *et al.*, "Heavy doping effects in Mg-doped GaN," *J. Appl. Phys.*, vol. 87, no. 4, pp. 1832–1835, 2000.

[5] V. Heera, D. Panknin, and W. Skorupa, "p-Type doping of SiC by high dose Al implantation-problems and progress," *Appl. Surf. Sci.*, vol. 184, nos. 1–4, pp. 307–316, 2001.

[6] Ü. Özgür *et al.*, "A comprehensive review of ZnO materials and devices," *J. Appl. Phys.*, vol. 98, no. 4, p. 041301, 2005.

[7] P. Ayala, R. Arenal, M. Rummeli, A. Rubio, and T. Pichler, "The doping of carbon nanotubes with nitrogen and their potential applications," *Carbon*, vol. 48, no. 3, pp. 575–586, 2010.

[8] G. Fiori *et al.*, "Electronics based on two-dimensional materials," *Nature Nanotechnol.*, vol. 9, no. 10, pp. 768–779, 2014.

[9] G. Gupta, B. Rajasekharan, and R. J. E. Hueting, "Electrostatic doping in semiconductor devices," *IEEE Trans. Electron Devices*, vol. 64, no. 8, pp. 3044–3055, Aug. 2017.

[10] K. Nadda and M. J. Kumar, "Vertical bipolar charge plasma transistor with buried metal layer," *Sci. Rep.*, vol. 5, Jan. 2015, Art. no. 7860.

[11] M. J. Kumar and S. Sharma, "GaAs tunnel diode with electrostatically doped n-region: Proposal and analysis," *IEEE Trans. Electron Devices*, vol. 62, no. 10, pp. 3445–3448, Oct. 2015.

[12] E. H. Rhoderick and R. H. Williams, *Metal-Semiconductor Contacts*, vol. 129. Oxford, U.K.: Clarendon, 1988.

[13] E. H. Rhoderick, "Comments on the conduction mechanism in Schottky diodes," *J. Phys. D, Appl. Phys.*, vol. 5, no. 10, p. 1920, Oct. 1972.

[14] W. H. Brattain and J. Bardeen, "Nature of the forward current in Germanium point contacts," *Phys. Rev.*, vol. 74, pp. 231–232, Jul. 1948.

[15] M. Wittmer, "Current transport in high-barrier IrSi/Si Schottky diodes," *Phys. Rev. B, Condens. Matter*, vol. 42, no. 8, pp. 5249–5259, Sep. 1990.

[16] M. Wittmer, "Conduction mechanism in PtSi/Si Schottky diodes," *Phys. Rev. B, Condens. Matter*, vol. 43, no. 5, p. 4385, Feb. 1991.

[17] *Sentaurus TCAD, Version l-2016.03 ed*, Synopsys Inc., Mountain View, CA, USA, 2016.

[18] D. B. M. Klaassen, "A unified mobility model for device simulation—I. Model equations and concentration dependence," *Solid-State Electron.*, vol. 35, no. 7, pp. 953–959, Jul. 1992.

[19] S. Sze and K. N. Kwok, *Physics of Semiconductor Devices*, 3rd ed. Hoboken, NJ, USA: Wiley, 2007.

[20] B. J. Baliga, "Analysis of a high-voltage merged p-i-n/Schottky (MPS) rectifier," *IEEE Electron Device Lett.*, vol. ED-8, no. 9, pp. 407–409, Sep. 1987.

[21] H. K. Gummel and H. C. Poon, "An integral charge control model of bipolar transistors," *Bell Syst. Tech. J.*, vol. 49, no. 5, pp. 827–852, May/Jun. 1970.

[22] D. Connelly, C. Faulkner, D. E. Grupp, and J. S. Harris, "A new route to zero-barrier metal source/drain MOSFETs," *IEEE Trans. Nanotechnol.*, vol. 3, no. 1, pp. 98–104, Mar. 2004.

[23] J. M. Andrews and M. P. Lepselter, "Reverse current-voltage characteristics of metal-silicide Schottky diodes," *Solid-State Electron.*, vol. 13, no. 7, pp. 1011–1023, Jul. 1970.

[24] P. G. McCafferty, A. Sellai, P. Dawson, and H. Elabd, "Barrier characteristics of PtSip-Si Schottky diodes as determined from *I-V-T* measurements," *Solid-State Electron.*, vol. 39, no. 4, pp. 583–592, Apr. 1996.

[25] C. R. Crowell and S. M. Sze, "Current transport in metal-semiconductor barriers," *Solid-State Electron.*, vol. 9, nos. 11–12, pp. 1035–1048, 1966.

[26] L. Qi, G. Lorito, and L. K. Nanver, "Lateral-transistor test structures for evaluating the effectiveness of surface doping techniques," *IEEE Trans. Semicond. Manuf.*, vol. 25, no. 4, pp. 581–588, Nov. 2012.

[27] X. Liu and L. K. Nanver, "Comparing current flows in ultra-shallow pn-/Schottky-like diodes with 2-diode test method," in *Proc. Int. Conf. Microelectron. Test Struct. (ICMTS)*, Mar. 2016, pp. 190–195.

[28] D. K. Schroder, *Semiconductor Material and Device Characterization*. Hoboken, NJ, USA: Wiley, 2006.

[29] A. R. Brown *et al.*, "SiGe fast-switching power diodes," in *IEDM Tech. Dig.*, Dec. 1998, pp. 699–702.

[30] K. R. C. Mok, L. Qi, A. H. G. Vlooswijk, and L. K. Nanver, "Self-aligned two-layer metallization with low series resistance for litho-less contacting of large-area photodiodes," *Solid-State Electron.*, vol. 111, pp. 210–217, Sep. 2015.

[31] D. L. Scharfetter, "Minority carrier injection and charge storage in epitaxial Schottky barrier diodes," *Solid-State Electron.*, vol. 8, no. 3, pp. 299–311, 1965.

[32] M. Alavi, D. K. Reinhard, and C. C. W. Yu, "Minority-carrier injection in Pt–Si Schottky-barrier diodes at high current densities," *IEEE Trans. Electron Devices*, vol. ED-34, no. 5, pp. 1134–1140, May 1987.

[33] E. F. Schubert, T. Gessmann, and J. K. Kim, *Light Emitting Diodes*. Hoboken, NJ, USA: Wiley, Jul. 2005.

[34] V. Puliyankot and R. J. E. Hueting, "One-dimensional physical model to predict the internal quantum efficiency of Si-based LEDs," *IEEE Trans. Electron Devices*, vol. 59, no. 1, pp. 26–34, Jan. 2012.

[35] D. A. B. Miller, "Device requirements for optical interconnects to silicon chips," *Proc. IEEE*, vol. 97, no. 7, pp. 1166–1185, Jul. 2009.

[36] Y. Wu *et al.*, "High efficiency single Ag nanowire/p-GaN substrate Schottky junction-based ultraviolet light emitting diodes," *Appl. Phys. Lett.*, vol. 106, no. 5, p. 051108, 2015.

[37] R. T. Tung, "The physics and chemistry of the Schottky barrier height," *Appl. Phys. Rev.*, vol. 1, no. 1, p. 011304, 2014.

[38] R. R. Lieten, V. V. Afanas'ev, N. H. Thoan, S. Degroote, W. Walukiewicz, and G. Borghs, "Mechanisms of Schottky barrier control on n-type germanium using Ge_3N_4 interlayers," *J. Electrochem. Soc.*, vol. 158, no. 4, pp. H358–H362, 2011.

[39] K. H. Kao and L. Y. Chen, "A dopingless FET with metal-insulator-semiconductor contacts," *IEEE Electron Device Lett.*, vol. 38, no. 1, pp. 5–8, Jan. 2017.

Gaurav Gupta received the B.Tech. degree in electrical engineering from IIT (BHU) Varanasi, Varanasi, India, in 2008, and the M.Sc. degree from The University of Manchester, Manchester, U.K., in 2009. He is currently pursuing the Ph.D. degree with the Semiconductor Components Group, MESA+ Institute for Nanotechnology, University of Twente, Enschede, The Netherlands.

His current research interests include semiconductor device physics and ultra-thin body based GaN devices.

Satadal Dutta (S'15) received the B.Tech. degree (Hons.) in electronics and electrical communication engineering and the M.Tech. degree in microelectronics and VLSI from IIT Kharagpur, Kharagpur, India, in 2013, and the Ph.D. degree from the MESA+ Institute for Nanotechnology, University of Twente, Enschede, The Netherlands, in 2017.

His current research interests include semiconductor device physics, optics, and optoelectronics.

Sourish Banerjee received the M.Sc. degree in electrical engineering from the Delft University of Technology, Delft, The Netherlands, in 2014. He is currently pursuing the Ph.D. degree from the University of Twente, Enschede, The Netherlands.

His current research interests include the growth and characterization of group III-nitride materials.

Raymond J. E. Hueting (S'94–M'98–SM'06) received the M.Sc. (*cum laude*) and Ph.D. degrees in electrical engineering from the Delft University of Technology, Delft, The Netherlands.

In 2005, he joined the Semiconductor Components Group, MESA+ Institute for Nanotechnology, University of Twente, Enschede, The Netherlands, where he has been involved in semiconductor device physics and modeling.